ACS Macro Letters

Letter

pubs.acs.org/macroletters

# Force–Extension for DNA in a Nanoslit: Mapping between the 3D and 2D Limits

Hendrick W. de Haan*,† and Tyler N. Shendruk‡

†University of Ontario Institute of Technology, Faculty of Science, 2000 Simcoe Street North, Oshawa, Ontario L1H 7K4, Canada

‡The Rudolf Peierls Centre for Theoretical Physics, Department of Physics, Theoretical Physics, University of Oxford, 1 Keble Road, Oxford, OX1 3NP, United Kingdom

Supporting Information

**ABSTRACT:** The force–extension relation for a semiflexible polymer confined in a nanoslit is investigated. Both the effective correlation length and force–extension relation change as the chain goes from 3D (large slit heights) to 2D (tight confinement). At low forces, correlations along the polymer give an effective dimensionality. The strong force limit can be interpolated with the weak force limit for two regimes: when confinement dominates over extensile force and vice versa. These interpolations give good agreement with simulations for all slit heights and forces. We thus generalize the Marko-Siggia force–extension relation for DNA and other semiflexible biopolymers in nanoconfinement.

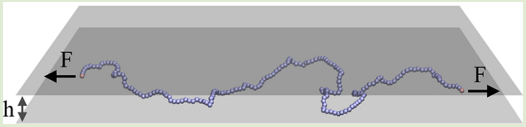


Many recent studies have focused on static[1−9] and dynamic[10−15] properties of semiflexible biopolymers, such as DNA, within nanoslits,[16,17] nanochannels,[18−21] and crowded environments.[22−24] Here, we study polymers of contour length $L_C$ confined within nanoslits and subjected to a stretching force $F$ with resulting extension $x$. We seek to generalize the Marko-Siggia (MS) force–extension relation (FER) to confined environments. Experimental examples include DNA stretched by electric fields in nanoslits[25] and tug-of-war or nanopit-type devices.[26−29] Both the 3D[30,31] and the 2D[32] limits of the FER have been studied extensively, but few studies investigate the crossover from 3D to 2D with confinement.[33] While scaling theories quite successfully predict conformations and dynamics of confined macromolecules,[34] a generalization of the FER[35] is needed. Chen et al. compared simulations to an FER proposed without derivation.[36] Since $x$ was defined as the distance between the ends in the direction of the force, the low-force regime was unresolved. We apply a force $\vec{F}_1 = F\hat{\hat{x}}$ (where $\hat{x}$ lies in the plane of the slit) to monomer 1, $\vec{F}_N = -F\hat{\hat{x}}$ to the last monomer and define $x = (\vec{r}_1 - \vec{r}_N) \cdot \hat{x}$. This ensures that $x \to 0$ as $F \to 0$, permitting exploration of the low-force regime.

We first find an explicit form of the MS-FER in $d$ discrete dimensions without explicit reference to polymer correlation length. We propose that this generalization can be applied to chains confined in nanochannels of height $h$ if a suitable effective dimensionality $d_{eff}$ is identified. For slits where $h$ is sufficiently small, $d_{eff} = 2$, while $d_{eff} = 3$ when $h$ is large. Intermediate values of $d_{eff}$ represent the impact of confinement on the FER and map between the 2D to 3D limits. Suitable low-force values arise from the confined correlation length, which can be interpolated with theoretical strong-force limits. By considering the competition between confinement and applied force, we derive the FER in two limits: confinement dominated and force dominated. Comparing with the MS-FER in discrete dimensions shows that the generalization can act as a semiempirical FER with an effective dimensionality $d_{eff}$ that depends on slit height and applied force.

Our results are substantiated by Langevin dynamics simulations of an ideal polymer of 200 monomers, with no interactions between non-neighboring monomers. The method used here follows standard implementations for a semiflexible polymer[37] and is described in detail in the Supporting Information (SI).

We now derive a generalized MS-FER for $d$ discrete dimensions. The FER can be approximated as the interpolation between the low- and strong-force limits. At low forces, we use the Kratky–Porod model[38] in $d$-dimensions, which describes the polymer as an entropic spring with extension $x/L_C = (2/d)(FL_\xi)/(k_BT)$ (see SI). This limit depends on $L_\xi$, the correlation length between tangent vectors. The correlation length is commonly referred to as persistence length but, to avoid ambiguity with the length scale of mechanical rigidity $L_\kappa = \kappa/k_BT$, we forego this term. While $L_\kappa$ is a thermomaterial property, $L_\xi$ depends on dimensionality. The two are not strictly equivalent.

In the strong-force limit, we utilize the equipartition theorem in Fourier space to find $x/L_C = 1 - ([d-1]/4) \times (k_BT/[FL_\kappa])^{1/2}$ (see SI). Interpolating between the limits produces a generalized MS-FER:

$$F = \frac{k_BT}{L_\kappa}\left(\frac{d-1}{4}\right)^2\left[\left(1-\frac{x}{L_C}\right)^{-2} - 1 + \left(\frac{d}{2}\left(\frac{4}{d-1}\right)^2\frac{L_\kappa}{L_\xi} - 2\right)\frac{x}{L_C}\right] \quad (1)$$

which is consistent with 3D[35] and 2D[32,39] forms.

**Received:** February 20, 2015
**Accepted:** May 11, 2015
**Published:** May 20, 2015

  

DOI: 10.1021/acsmacrolett.5b00138
*ACS Macro Lett.* 2015, 4, 632–635

Reasonable agreement with simulations in 3D (indistinguishable from $h = 199$) is obtained for $d = 3$ and $L_\xi = L_\kappa$ (Figure 1). The slight overprediction in the 3D limit is a limitation of the simulations (see SI).

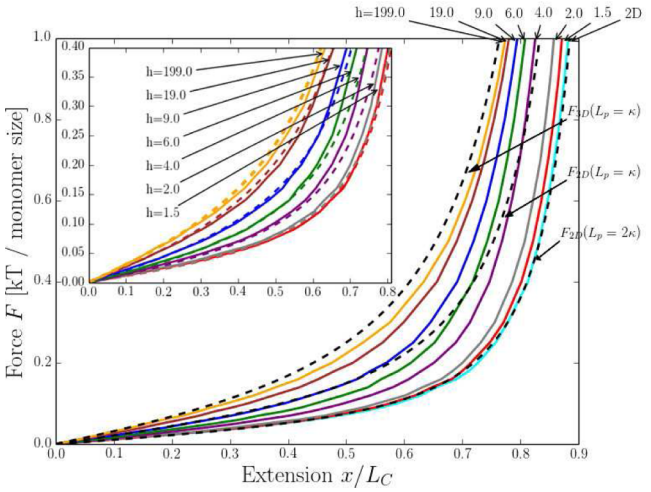


**Figure 1.** Simulated force−extension relation for various slit heights. Dashed lines indicate theoretical curves (eq 1). In 2D, the curves using both $L_\xi = L_\kappa$ and $L_\xi = 2L_\kappa$ are shown.

The 2D FER is shifted to larger extensions compared to 3D (Figure 1). Equation 1 fails to agree with the simulations if $L_\kappa$ is erroneously utilized as $L_\xi$ (appropriate only in 3D). Not only do the coefficients of the MS-FER change but

$$L_\xi(L_\kappa, d) = \frac{2L_\kappa}{d-1} \tag{2}$$

does as well as previously stated[40] and is explicitly verified in SI. In 2D, $L_\xi = 2L_\kappa$.

Substituting $L_\xi$ into eq 1 produces the generalized MS-REF without reference to correlation length

$$F(x, d) = \frac{k_B T}{L_\kappa}\left(\frac{d-1}{4}\right)^2\left[\left(1-\frac{x}{L_C}\right)^{-2} - 1 + 2\left(\frac{d+1}{d-1}\right)\frac{x}{L_C}\right] \tag{3}$$

which is in excellent agreement with both the 3D and 2D limits (Figure 1).

Equation 3 represents a unified form of the FER for discrete dimensions. It also suggests that confinement-induced crossover from 3D to 2D can be discussed in terms of an effective dimensionality $2 \le d_{eff} \le 3$. The polymer does not exist in a fractional dimension but rather a continuous effective dimensionality quantifies the extent to which confinement alters the FER.

We use eq 2 to define the low-force limit to be $d_{eff} \to d_{eff}^{low} = 1 + 2L_\kappa/L_\xi(h)$. The correlation length is typically measured via $\langle \cos \theta_{i,i+\delta i}\rangle$ for the angle $\theta_{i,i+\delta i}$ between segments $i$ and $i + \delta i$ using $\langle \cos \theta_{i,i+\delta i}\rangle \equiv e^{-\delta i/L_\xi}$. While this approach works well in 2D and 3D, the results for intermediate heights are nonisotropic (Figure 2, inset). At intermediate heights, the parallel components remain monotonically positive, but the perpendicular component does not. Fully understanding the correlation functions of semiflexible polymers in confinement remains challenging experimentally,[41−44] computationally,[45−47] and analytically.[48−50]

Following Chen et al.,[36] we use parallel correlation measurements to define $L_\xi(h)$, which crosses over from 3D to 2D with decreasing slit height (Figure 2). The black solid line is a fit for $h \le 2\ L_\kappa$ given by

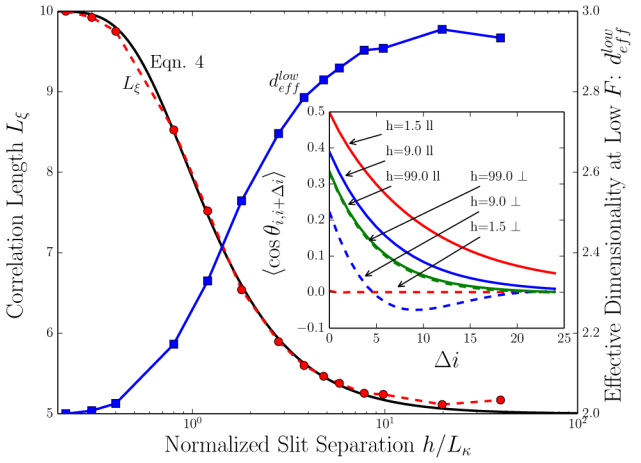


**Figure 2.** Correlation length (dashed circles) and corresponding effective dimensionality (solid squares) as a function of the slit height. Solid black lines fit the data for $h \le 2L_\kappa$ (eq 4). Inset shows the components of correlations of direction vectors along the polymer contour.

$$L_\xi(L_\kappa, h) = L_\kappa\left[2 - e^{-0.88(L_\kappa/h)^{1.41}}\right] \tag{4}$$

which agrees with theory for both $h \to 0$ and $h \to \infty$. Correspondingly, $d_{eff}^{low}(L_\xi/L_\kappa)$ varies smoothly from 3 to 2.

We propose that $d_{eff}$ can be substituted into eq 3 in place of the discrete dimensionality $d$ to produce a semiempirical FER for confined polymers. For now, we assume $d_{eff}$ is only a function of $L_\xi$. This allows eq 3 to apply to finite slit confinements as a function of measured $L_\xi$ (Figure 1, inset).

Good agreement is obtained for moderate extensions. Hence, the $d_{eff}$ approach maps the crossover from 3D to 2D at low forces. However, the theory overpredicts the large-extension regime in comparison to simulations (Figure 1, inset). This suggests that expressing extension in terms of $d_{eff}$ is only accurate for low forces

$$\lim_{F \ll k_B T/L_\kappa} \frac{x}{L_C} = \frac{4FL_\kappa}{d_{eff}^{low}(d_{eff}^{low} - 1)k_B T} \tag{5}$$

Since taut, confined polymers can only accommodate small thermal fluctuations about the line connecting their ends,[51] they feel the effect of the walls less. Hence, confinement effects diminish as force increases, causing $d^{eff}$ to increase. Confining walls act to cut off the lowest frequencies allowed in Fourier space, which increases the average extension (see SI). We find the expression for the extension in the strong force limit and arbitrary slit confinement to be

$$\lim_{F \gg k_B T/L_\kappa} \frac{x}{L_C} = 1 - \frac{1}{2}\sqrt{\frac{k_B T}{FL_\kappa}}\left[1 - \frac{1}{\pi}\tan^{-1}\left(c_0\frac{h}{L_\kappa}\sqrt{\frac{k_B T}{FL_\kappa}}\right)\right] \tag{6}$$

where $c_0$ controls the cutoff. This general form for the strong-force FER is in good agreement with the high-force limit of the simulations for all slit heights.

Interpolating between eqs 5 and 6 is not possible for arbitrary confinement, and we must consider the argument of the arctangent in eq 6. We expand the confinement-dominated $h/L_\kappa \ll (k_B T/[FL_\kappa])^{1/2}$ and force dominated $h/L_\kappa \gg (k_B T/[FL_\kappa])^{1/2}$ cases. Interpolation can be found separately in either



DOI: 10.1021/acsmacrolett.5b00138
ACS Macro Lett. 2015, 4, 632−635

limit. Interpolating the force-dominated limit of the strong-force regime with eq 5 gives

$$F = \frac{k_B T}{4L_\kappa}\left[\left(1 - \frac{x}{L_C}\right)^{-2} - 8c_0\frac{L_\kappa}{h}\left(1 - \frac{x}{L_C}\right)^{-1} - \left(1 - 8c_0\frac{L_\kappa}{h}\right) + 2\left\{\frac{d_{\text{eff}}^{\text{low}}(d_{\text{eff}}^{\text{low}} - 1)}{2} - \left(1 - 4c_0\frac{L_\kappa}{h}\right)\right\}\frac{x}{L_C}\right] \quad (7)$$

The cutoff $c_0 = 0.3$ is acceptable and eq 7 is highly accurate at both low and high forces when $h \gtrsim L_\kappa$ (Figure 3). However, the weak confinement approximation breaks down as slit height decreases.

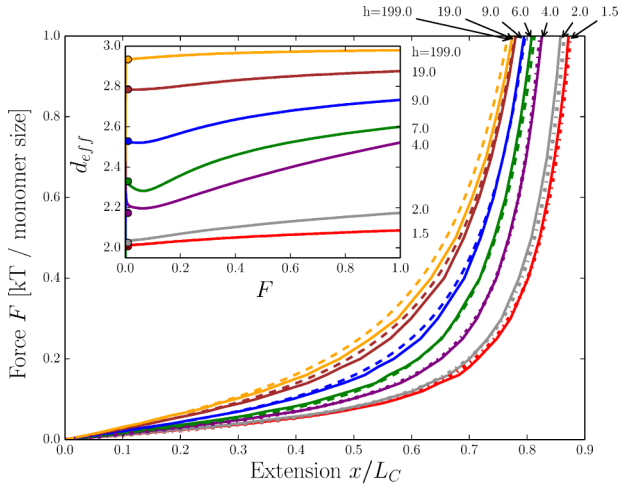


**Figure 3.** Simulated force extension curves (solid lines) and eq 7 for $h > L_\kappa$ (dashed lines) or eq 8 for $h < L_\kappa$ (dash-dot lines). Inset shows the dependence of effective dimensionality on force for different slit heights. Circles indicate $d_{\text{eff}}^{\text{low}}$ values.

The other limit of eq 6 is confinement dominated. Interpolating the confinement-dominated limit with eq 5 produces

$$F = \frac{k_B T}{16L_\kappa}\left[\left(1 - \frac{x}{L_c} - \frac{1}{2\pi c_0}\frac{h}{L_\kappa}\right)^{-2} - \left(1 + \frac{1}{\pi c_0}\frac{h}{L_\kappa}\right) + 2(2d_{\text{eff}}^{\text{low}2} - 2d_{\text{eff}}^{\text{low}} - 1)\frac{x}{L_C}\right] \quad (8)$$

where $c_0 = 1.55$ to obtain acceptable agreement. Figure 3 demonstrates that this interpolation is accurate for $h \lesssim L_\kappa$.

The relative error of the interpolations (eq 7 or 8) with the simulations is $(F_i(h,x) - F_s(h,x))/F_s(h,x)$ (Figure 4). For moderate to tight confinement, the relative error is generally within ±5%. Since the results diverge in 3D due to simulation limitations (see SI), the relative error is large for weak confinement. However, the dashed black line is the relative error between the 3D limit of eq 7 and the 3D MS-FER, confirming eq 7 approaches the proper 3D limit.

Having generalized the interpolations for force extension in a slit, we return to the effective dimensionality in eq 3, now recognizing that $d_{\text{eff}}$ depends on both slit height and force. We extract $d_{\text{eff}}(F,h)$ by fitting eq 3 to the analytical eqs 7 and 8 (Figure 3, inset). The full $d_{\text{eff}}$ shows how the effect of confinement decays with both increasing $h$ and $F$ as the curves move from 2D to 3D. Further, $d_{\text{eff}}$ demonstrates quantitatively

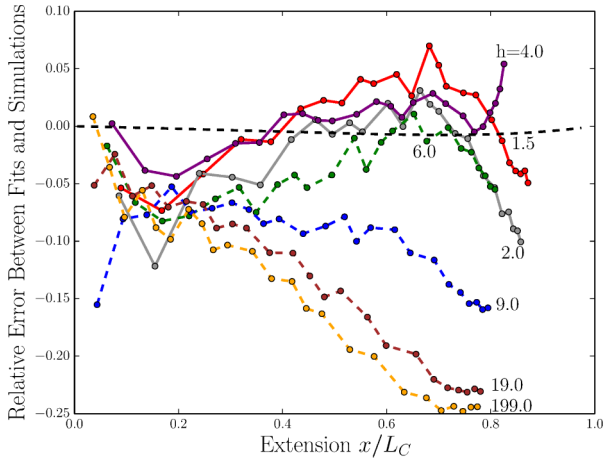


**Figure 4.** Relative error between simulation results and the interpolation formula given by eq 7 for $h > L_\kappa$ (dashed lines) or eq 8 for $h < L_\kappa$ (solid lines). The dashed black line is the difference between eq 7 at $d_{\text{eff}}^{\text{low}} = 3$ and the 3D Marko-Siggia relation.

that the force dependence is dramatic at intermediate heights but otherwise weak.

In conclusion, we have presented a physical picture of the force−extension relation (FER) for DNA confined within nanoslits by introducing an effective dimensionality, $d_{\text{eff}}$. Using $d_{\text{eff}}$ in a generalized Marko-Siggia FER leads to good agreement with simulations for all slit heights and forces. At low forces, $d_{\text{eff}}$ is determined from in-plane correlations. However, the effect of confinement is reduced for larger forces. Via interpolation, we derived FERs for force-dominated (near 3D) and confinement-dominated (near 2D) systems. These formulas give good agreement with all simulation results. Comparison to the generalized Marko-Siggia yields $d_{\text{eff}}$ as a function of both slit height and stretching force. For tight confinements, $d_{\text{eff}} \to 2$ but tends toward 3 as slit height increases. The effective dimensionality thus provides as a useful physical perspective on force−extension curves for biopolymers subject to natural and artificial confinement.

## ■ ASSOCIATED CONTENT

### Ⓢ Supporting Information

Detailed description of simulation method. Simulations of $N = \{300, 400\}$ at $h = 19.0$ verifying no appreciable difference in the force−extension curves. Mathematical derivations of the correlation length, and the weak- and strong-force limits in $d$-dimensions subject to confinement. The Supporting Information is available free of charge on the ACS Publications website at DOI: 10.1021/acsmacrolett.5b00138.

## ■ AUTHOR INFORMATION

### Corresponding Author

*E-mail: hendrick.dehaan@uoit.ca.

### Notes

The authors declare no competing financial interest.

## ■ ACKNOWLEDGMENTS

Simulations performed using HOOMD Blue[52] on SHARCNET (www.sharcnet.ca). The authors gratefully acknowledge useful discussions with Alexander R. Klotz and EMBO funding to T.N.S. (ALTF181-2013).



DOI: 10.1021/acsmacrolett.5b00138
ACS Macro Lett. 2015, 4, 632−635

## REFERENCES


(1) Lin, P.-K.; Fu, C.-C.; Chen, Y.-L.; Chen, Y.-R.; Wei, P.-K.; Kuan, C. H.; Fann, W. S. *Phys. Rev. E* **2007**, *76*, 011806.
(2) Dimitrov, D. I., Milchev, A., Binder, K., Klushin, L. I., Skvortsov, A. M. *J. Chem. Phys.*. **2008***128*.
(3) Cifra, P.; Benková, Z.; Bleha, T. *J. Phys. Chem. B* **2009**, *113*, 1843−1851.
(4) Tang, J.; Trahan, D. W.; Doyle, P. S. *Macromolecules* **2010**, *43*, 3081−3089.
(5) Dai, L.; Jones, J. J.; van der Maarel, J. R. C.; Doyle, P. S. *Soft Matter* **2012**, *8*, 2972−2982.
(6) Cifra, P. *J. Chem. Phys.*. **2012***136*.
(7) Hsu, H.-P.; Binder, K. *Macromolecules* **2013**, *46*, 8017−8025.
(8) Chen, Y.-L.; Lin, Y.-H.; Chang, J.-F.; Lin, P.-k *Macromolecules* **2014**, *47*, 1199−1205.
(9) Benkova, Z.; Namer, P.; Cifra, P. *Soft Matter* **2015**, *11*, 2279−2289.
(10) Hsieh, C.-C.; Balducci, A.; Doyle, P. S. *Macromolecules* **2007**, *40*, 5196−5205.
(11) Strychalski, E. A.; Levy, S. L.; Craighead, H. G. *Macromolecules* **2008**, *41*, 7716−7721.
(12) Tang, J.; Levy, S. L.; Trahan, D. W.; Jones, J. J.; Craighead, H. G.; Doyle, P. S. *Macromolecules* **2010**, *43*, 7368−7377.
(13) Milchev, A. *J. Phys.: Condens. Matter* **2011**, *23*, 103101.
(14) Trahan, D. W.; Doyle, P. S. *Macromolecules* **2011**, *44*, 383−392.
(15) Dai, L.; Tree, D. R.; van der Maarel, J. R. C.; Dorfman, K. D.; Doyle, P. S. *Phys. Rev. Lett.* **2013**, *110*, 168105.
(16) Jo, K.; Dhingra, D. M.; Odijk, T.; de Pablo, J. J.; Graham, M. D.; Runnheim, R.; Forrest, D.; Schwartz, D. C. *Proc. Natl. Acad. Sci. U.S.A.* **2007**, *104*, 2673−2678.
(17) Orlandini, E.; Micheletti, C. *J. Biol. Phys.* **2013**, *39*, 267−275.
(18) Reisner, W.; Morton, K. J.; Riehn, R.; Wang, Y. M.; Yu, Z.; Rosen, M.; Sturm, J. C.; Chou, S. Y.; Frey, E.; Austin, R. H. *Phys. Rev. Lett.* **2005**, *94*, 196101.
(19) Tree, D. R.; Wang, Y.; Dorfman, K. D. *Phys. Rev. Lett.* **2013**, *110*, 208103.
(20) Tree, D. R.; Wang, Y.; Dorfman, K. D. *Biomicrofluidics* **2013**, *7*, 054118.
(21) Vázquez-Montejo, P.; McDargh, Z.; Deserno, M.; Guven, J. *arXiv preprint arXiv:1503.01023* **2015**.
(22) Shin, J.; Cherstvy, A. G.; Metzler, R. *New J. Phys.* **2014**, *16*, 053047.
(23) Shin, J.; Cherstvy, A. G.; Metzler, R. *ACS Macro Lett.* **2015**, *4*, 202−206.
(24) Shendruk, T. N.; Bertrand, M.; de Haan, H. W.; Harden, J. L.; Slater, G. W. *Biophys. J.* **2015**, *108*, 810−820.
(25) Sriram, K. K.; Y.C, Y. L.; Yeh, J. W.; Chou, C. *Nucleic Acids Res.* **2014**, *42*, e85.
(26) Reisner, W.; Larsen, N. B.; Flyvbjerg, H.; Tegenfeldt, J. O.; Kristensen, A. *Proc. Natl. Acad. Sci. U.S.A.* **2009**, *106*, 79−84.
(27) Klotz, A. R.; Brandão, H. B.; Reisner, W. W. *Macromolecules* **2012**, *45*, 2122−2127.
(28) Yeh, J.-W.; Taloni, A.; Chen, Y.-L.; Chou, C.-F. *Nano Lett.* **2012**, *12*, 1597−1602.
(29) Kounovsky-Shafer, K. L.; Hernández-Ortiz, J. P.; Jo, K.; Odijk, T.; de Pablo, J. J.; Schwartz, D. C. *Macromolecules* **2013**, *46*, 8356−8368.
(30) Bustamante, C.; Smith, S. B.; Liphardt, J.; Smith, D. *Curr. Opin. Struct. Biol.* **2000**, *10*, 279−285.
(31) Bustamante, C.; Bryant, Z.; Smith, S. B. *Nature* **2003**, *421*, 423−427.
(32) Hsu, H.-P.; Paul, W.; Binder, K. *Europhys. Lett.* **2011**, *95*, 68004.
(33) Taloni, A.; Yeh, J.-W.; Chou, C.-F. *Macromolecules* **2013**, *46*, 7989−8002.
(34) Tree, D. R.; Reinhart, W. F.; Dorfman, K. D. *Macromolecules* **2014**, *47*, 3672−3684.
(35) Marko, J. F.; Siggia, E. D. *Macromolecules* **1995**, *28*, 8759−8770.
(36) Chen, Y.-L.; Lin, P.-k.; Chou, C.-F. *Macromolecules* **2010**, *43*, 10204−10207.
(37) Slater, G. W.; Holm, C.; Chubynsky, M. V.; de Haan, H. W.; Dubé, A.; Grass, K.; Hickey, O. A.; Kingsburry, C.; Sean, D.; Shendruk, T. N.; Zhan, L. *Electrophoresis* **2009**, *30*, 792−818.
(38) Kratky, O.; Porod, G. *Rec. Trav. Chim. Pays-Bas* **1949**, *68*, 1106−1122.
(39) Prasad, A.; Hori, Y.; Kondev, J. *Phys. Rev. E* **2005**, *72*, 041918.
(40) Huang, A.; Adhikari, R.; Bhattacharya, A.; Binder, K. *Europhys. Lett.* **2014**, *105*, 18002.
(41) Köster, S.; Steinhauser, D.; Pfohl, T. *J. Phys.: Condens. Matter* **2005**, *17*, S4091.
(42) Köster, S.; Stark, H.; Pfohl, T.; Kierfeld, J. *Biophys. Rev. Lett.* **2007**, *02*, 155−166.
(43) Köster, S.; Kierfeld, J.; Pfohl, T. *Eur. Phys. J. E* **2008**, *25*, 439−449.
(44) Nöding, B.; Köster, S. *Phys. Rev. Lett.* **2012**, *108*, 088101.
(45) Cifra, P.; Benková, Z.; Bleha, T. *J. Phys. Chem. B* **2008**, *112*, 1367−1375.
(46) Cifra, P.; Benkova, Z.; Bleha, T. *Faraday Discuss.* **2008**, *139*, 377−392.
(47) Benková, Z.; Cifra, P. *Macromolecules* **2012**, *45*, 2597−2608.
(48) Harnau, L.; Reineker, P. *Phys. Rev. E* **1999**, *60*, 4671−4676.
(49) Choi, M. C.; Santangelo, C. D.; Pelletier, O.; Kim, J. H.; Kwon, S. Y.; Wen, Z.; Li, Y.; Pincus, P. A.; Safinya, C. R.; Kim, M. W. *Macromolecules* **2005**, *38*, 9882−9884.
(50) Wagner, F.; Lattanzi, G.; Frey, E. *Phys. Rev. E* **2007**, *75*, 050902.
(51) Baba, T.; Sakaue, T.; Murayama, Y. *Macromolecules* **2012**, *45*, 2857−2862.
(52) Anderson, J. A.; Lorenz, C. D.; Travesset, A. *J. Comput. Phys.* **2008**, *227*, 5342−5359.




DOI: 10.1021/acsmacrolett.5b00138
*ACS Macro Lett.* 2015, 4, 632−635